Effect of axial prestretch on inflation instability in finitely extensible thin-walled tube

L. Horný

***Abstract*—Mechanical response of elastic materials undergoing large deformations exhibit several kinds of a loss of stability. Such a situation may occur, for instance, when a thin-walled cylinder is inflated by an internal pressure. The loss of stability is manifested by a non-monotonic relationship between the inflating pressure and the circumferential stretch of the tube. The results, known from the literature, show that hyperelastic materials with so called *limiting chain extensibility* property always exhibit a stable response for sufficiently small values of the limiting extensibility parameter J_m. In other words, rapid large strain stiffening prevents elastomeric materials from an onset of instability. The present study demonstrates how axial prestretch of the thin-walled tube affects the stability of the deformation. It is shown that for axial prestretches λ_z = 1 (non-prestretched), 1.05, 1.1, 1.2, 1.5, 2, 3, and 5 the stable inflation is obtained for materials with J_m = 19.11, 20.32, 21.55, 24.06, 32.1, 47.43, 87.23, and 207.8, respectively. From which can be concluded that the higher the prestretch is, the more compliant material will show stable inflation. It was also found that the higher the prestretch is, the lower is the pressure at which the instability occurs.**

***Index Terms*—Axial prestretch, Hyperelasticity, Inflation instability, Limiting chain extensibility, Pressurization.**

I. Introduction

MATERIALS undergoing large elastic deformations exhibit many non-self-evident phenomena in their mechanical behavior. Some of them are linked to a loss of stability during deformation. For instance, non-monotonic inflation of thin-walled cylinders and spheres, kink formation on a twisted rod, or wrinkling of the surface of the bent block are good examples [1-4]. Traditionally, they have been discussed with reference to rubber-like materials; however, possible applications to the mechanics of soft tissues (arteries, veins, skin), which inherently undergoing large deformations, has also been recently recognized [4-10].

A typical example is the instability of a pressurized thin-walled cylindrical tube, which can manifest in two different ways. The first is the onset of buckling instability manifested by a transverse deflection (in the biomechanics of blood vessels this is usually referred to as tortuosity) similar to the buckling seen in a long slender column [6-10]. H.C. Han and coworkers investigated this problem in detail and developed mathematical expressions relating critical pressure to axial load, torsion couple, and geometry [6, 8-10].

Another mechanism by which pressurized tubes become unstable is through non-monotonic inflation [1, 2, 11-15]. It is a well-known phenomenon to all who have inflated a party-balloon. In this situation the radius of the balloon monotonically increases in contrast to applied pressure. The balloon appears to be stiff at initial deformations, however, the pressure-stretch relationship reaches a local maximum at a certain deformation. After the local maximum is passed, the pressure-stretch relationship forms a decreasing function and may reach a local minimum, which can be followed again by an increasing function, depending on the constitutive model used. In experiments, non-monotonic inflation may be accompanied with localized deformation (bulging – a loss of constant radius along the axis of the tube) which resembles aneurysm formation in arteries [12-15].

Non-monotonic inflation is one of the most studied instabilities in the context of rubber-like materials and will be of our concern. We will focus on the behavior of thin-walled cylindrical tubes with closed ends made from a material undergoing rapid large strain stiffening. Kanner and Horgan [2] recently investigated this problem in isotropic hyperelastic tubes exhibiting *limiting chain extensibility*. *Limiting chain extensibility* involves statistical polymer mechanics that explain large strain stiffening of elastomer materials based on the finite extensibility of macromolecular chains. In [2], a phenomenological analogue of molecular models based on a logarithmic form of the strain energy density function, which was originally proposed by A.N. Gent [16] (see also [17] for molecular statistical interpretation, and [18, 19] for details of the application in arterial biomechanics), was used.

It has been shown that, depending on the specific value of the limiting extensibility parameter J_m, non-monotonic inflation of thin-walled cylindrical tubes may or may not occur [2]. To be more specific, cylindrical tubes made from the material with $J_m < 18.2$ are always stable during a pressurization and tubes with $J_m > 18.2$ exhibit local maximum followed by local minimum.

Kanner and Horgan [2] investigated tubes operating in their natural state – that is without any axial force except the force induced by the pressure acting on the closed ends of the tube. There are, however, situations when tubes are axially

Manuscript received August 10, 2014 and accepted for publication September 22, 2014. This work has been supported by the Czech Ministry of Health in the project no. NT 13302.

Lukáš Horný is with the Faculty of Mechanical Engineering, Czech Technical University in Prague, Technická 4, 166 07, Prague, Czech Republic. Tel.: +420 22435 2542, email: lukas.horny@fs.cvut.cz

prestretched in a mounting. One nice example are blood vessels. In our bodies, arteries are longitudinally prestrained. This fact, although known since 1880 due to Roy [20], did not receive large scientific attention in comparison with the circumferential stiffness and distensibility of arteries, but at present its significant physiological role comes to light [19, 21-27].

In the present study, the effect of axial prestretch on the inflation instability will be investigated from two points of view. It will be shown that axial prestretch enables materials with $J_m > 18.2$ to be stable in the inflation. For one specific J_m ($J_m = 25$), it will be also shown that increased prestretch leads to the decreased internal pressure in the onset of the instability.

II. METHODS

A. Constitutive model

The material of the tube will be considered to be incompressible and hyperelastic characterized by the strain energy function W defined per unit reference volume. In such a case the constitutive equation can be written in the form (1) [28].

$$\boldsymbol{\sigma} = -p\,\mathbf{I} + \frac{\partial W}{\partial \mathbf{F}}\mathbf{F}^T \tag{1}$$

Here $\boldsymbol{\sigma}$ denotes the Cauchy stress tensor. $\mathbf{F}$ is the deformation gradient defined as $\mathbf{F} = \partial \boldsymbol{x}/\partial \boldsymbol{X}$, where $\boldsymbol{x}$ and $\boldsymbol{X}$, respectively, denote the position vector of a material particle in the deformed and the reference configuration. p plays the role of a Lagrangean multiplier, which represents the hydrostatic contribution to $\boldsymbol{\sigma}$, not captured by W, due to the incompressibility constraint.

Over the last decades, several models for W have been developed to describe the mechanical behavior of elastomers and soft tissues under large strains. We will focus ourselves on the so called *limiting chain extensibility* model proposed by Gent in 1996 [16]. It will be used in the form (2) which has appeared in the studies of arterial mechanics [18,19].

$$W = -\frac{\mu J_m}{2}\ln\left(1 - \frac{I_1 - 3}{J_m}\right) \tag{2}$$

Here μ is the shear modulus at infinitesimal strains. I_1 denotes the first invariant of the right Cauchy-Green strain tensor $\mathbf{C}$ ($I_1 = trace(\mathbf{C})$), where $\mathbf{C} = \mathbf{F}^T\mathbf{F}$ (alternatively one can also use left Cauchy-Green strain tensor $\mathbf{b}$, $\mathbf{b} = \mathbf{F}\mathbf{F}^T$, because $I_1(\mathbf{C}) = I_1(\mathbf{b})$). J_m is referred to as the *limiting extensibility* (dimensionless) *parameter* because it restricts admissible deformations of the material to the domain where $I_1 - 3 < J_m$ applies. In other words, $I_1 - 3 \to J_m^-$ implies $W \to \infty$. Thus finite extensibility of a macromolecular chain is, in the phenomenological approach, captured by a suitable mathematical form of the strain energy (logarithmic function).

Regarding inflation instability, Kanner and Horgan [2] found that there is a critical value of J_m, $J_m = 18.2$, which discriminates behaviors of pressurized thin-walled cylindrical tubes. The inflation is stable (monotonically increasing pressure for increasing circumferential stretch) for materials with $J_m < 18.2$. Whereas for materials with $J_m > 18.2$, there is a local maximum followed by local minimum that is subsequently followed by a steeply increasing section of the pressure-stretch curve (see Figure 5 in [2]). Substituting from (2) into (1) one obtains constitutive equations in the form (3).

$$\boldsymbol{\sigma} = \mu\frac{J_m}{J_m - (I_1 - 3)}\mathbf{b} - p\mathbf{I} \tag{3}$$

B. Inflation-extension of the thin-walled tube

Consider a long thin-walled cylindrical tube with closed ends that, in the reference configuration, has a middle radius R, thickness H, and length L. Assume that during pressurization, the motion of the material particle located originally at (R, Θ, Z), which is sufficiently distant from ends, is described by the equations summarized in (4).

$$r = \lambda_\theta R \qquad h = \lambda_r H \qquad z = \lambda_z Z \qquad \theta = \Theta \tag{4}$$

Here r and h respectively denote deformed middle radius and thickens. The equations (4) express the fact that the tube is uniformly inflated and extended (or shortened) and that it is not twisted. The stretches λ_k ($k = r, \theta, z$) are the components of the deformation gradient $\mathbf{F}$, $\mathbf{F} = diag[\lambda_r, \lambda_\theta, \lambda_z]$, and for the right Cauchy-Green strain tensor $\mathbf{C} = diag[\lambda_r^2, \lambda_\theta^2, \lambda_z^2]$ applies. In this kinematics, the invariant I_1 has the form (5).

$$I_1 = \lambda_r^2 + \lambda_\theta^2 + \lambda_z^2 \tag{5}$$

The material of the tube is considered to be incompressible, thus the volume ratio J, $J = det(\mathbf{F})$, gives equation (6) expressing $J = 1$.

$$\lambda_r\,\lambda_\theta\,\lambda_z = 1 \tag{6}$$

Equilibrium equations of a thin-walled tube with closed ends loaded by an internal pressure P and axial (prestretching) force F_{red} can be written in the form (7). Here σ_r, σ_θ, and σ_z respectively, denote the radial, circumferential and axial component of the Cauchy stress tensor.

$$\sigma_r = -\frac{P}{2} \qquad \sigma_\theta = \frac{rP}{h} \qquad \sigma_z = \frac{F_{red}}{2\pi rh} + \frac{rP}{2h} \tag{7}$$

The combination of constitutive equation (3), I_1 (5), and equilibrium equations (7) gives the system of equations governing the inflation-extension response (8–9).

$$\mu J_m \frac{\lambda_r^2}{J_m-\lambda_r^2-\lambda_\theta^2-\lambda_z^2+3}-p=-\frac{P}{2} \tag{8}$$

$$\mu J_m \frac{\lambda_\theta^2}{J_m-\lambda_r^2-\lambda_\theta^2-\lambda_z^2+3}-p=\frac{Pr}{h} \tag{9}$$

$$\mu J_m \frac{\lambda_z^2}{J_m-\lambda_r^2-\lambda_\theta^2-\lambda_z^2+3}-p=\frac{Fred}{2\pi rh}+\frac{Pr}{2h} \tag{10}$$

From the first equation, (9), it can be concluded that the Lagrangean multiplier p has the form (11).

$$p=\mu J_m \frac{\lambda_r^2}{J_m-\lambda_r^2-\lambda_\theta^2-\lambda_z^2+3}+\frac{P}{2} \tag{11}$$

Now we will substitute (11) into (9) and (10). Prior doing so, the application of the equations (4a) and (4b) enable us to work with known reference geometry. Bearing in mind the incompressibility condition (6), we also eliminate explicit dependence on λ_r, $\lambda_r = 1/\lambda_\theta/\lambda_z$. After some simple algebra, we arrive at equations governing the inflation-extension response: (12) for circumferential direction, and (13) for axial direction.

$$\mu J_m \frac{\lambda_\theta^2}{J_m-\frac{1}{\lambda_\theta^2\lambda_z^2}-\lambda_\theta^2-\lambda_z^2+3}-\mu J_m \times \\ \times\frac{1}{\left(J_m-\frac{1}{\lambda_\theta^2\lambda_z^2}-\lambda_\theta^2-\lambda_z^2+3\right)\lambda_\theta^2\lambda_z^2}-\frac{P}{2}=\frac{PR\lambda_\theta^2\lambda_z}{H} \tag{12}$$

$$\mu J_m \frac{\lambda_z^2}{J_m-\frac{1}{\lambda_\theta^2\lambda_z^2}-\lambda_\theta^2-\lambda_z^2+3}-\mu J_m \times \\ \times\frac{1}{\left(J_m-\frac{1}{\lambda_\theta^2\lambda_z^2}-\lambda_\theta^2-\lambda_z^2+3\right)\lambda_\theta^2\lambda_z^2}-\frac{P}{2}=\frac{\lambda_z Fred}{2\pi RH}+ \\ +\frac{PR\lambda_\theta^2\lambda_z}{2H} \tag{13}$$

As the final step, the equations (12) and (13) will be divided by μ to obtain dimensionless pressure. In (14) and (15), the notation $\varepsilon = H/R$ is also introduced.

$$J_m \frac{\lambda_\theta^2}{J_m-\frac{1}{\lambda_\theta^2\lambda_z^2}-\lambda_\theta^2-\lambda_z^2+3}- \\ J_m \frac{1}{\left(J_m-\frac{1}{\lambda_\theta^2\lambda_z^2}-\lambda_\theta^2-\lambda_z^2+3\right)\lambda_\theta^2\lambda_z^2}-\frac{P}{2\mu}=\frac{P}{\mu}\frac{\lambda_\theta^2\lambda_z}{\varepsilon} \tag{14}$$

$$J_m \frac{\lambda_z^2}{J_m-\frac{1}{\lambda_\theta^2\lambda_z^2}-\lambda_\theta^2-\lambda_z^2+3}- \\ J_m \frac{1}{\left(J_m-\frac{1}{\lambda_\theta^2\lambda_z^2}-\lambda_\theta^2-\lambda_z^2+3\right)\lambda_\theta^2\lambda_z^2}-\frac{P}{2\mu}= \\ \frac{\lambda_z Fred}{2\pi R^2\varepsilon\mu}+\frac{P}{\mu}\frac{\lambda_\theta^2\lambda_z}{2\varepsilon} \tag{15}$$

C. Simulation of the inflation-extension response

The equations (14) and (15) will be used to simulate mechanical response of internally pressurized and axially prestretched thin-walled tube. The simulations will show how axial prestretch affects circumferential stretch and internal pressure at the onset of instability (**SIM 1**), and that imposing of the prestretch elevates the value of J_m which discriminates between stable and unstable mechanical response of the tube (**SIM 2**).

All the computations were performed numerically in the computer algebra system MAPLE 18 using the command *fsolve* and incrementing λ_θ by 0.001. The simulations were conducted in two steps. In the first step, initial circumferential stretch λ_θ^{ini} and prestretching axial force F_{red} were solved with prescribed axial prestretch λ_z^{ini} and internal pressure $P = 0$. In the second step, λ_θ was incremented whereas F_{red} hold constant, and unknown P and λ_z were obtained by the *fsolve* procedure.

SIM1 was performed for λ_z^{ini} = 1, 1.01, 1.025, 1.05, 1.075, 1.1, 1.15, 1.2, 1.23 and 1.3 with J_m = 25. In **SIM2**, λ_z^{ini} = 1, 1.1, 1.2, 1.5, 2, 3, and 5 were used and J_m was incremented from 18.2 to the value at which local maximum appeared for the first time. In **SIM2**, four significant digits were considered in the procedure.

III. Results and Discussion

Predicted inflation-extension responses for **SIM1** are in the Figure 1 ($P/\mu - \lambda_\theta$ in the panel A, and $P/\mu - \lambda_z$ in B). The Figure 2 depicts the results obtained in SIM2 ($P/\mu - \lambda_\theta$ in the panel A, and $P/\mu - \lambda_z$ in B).

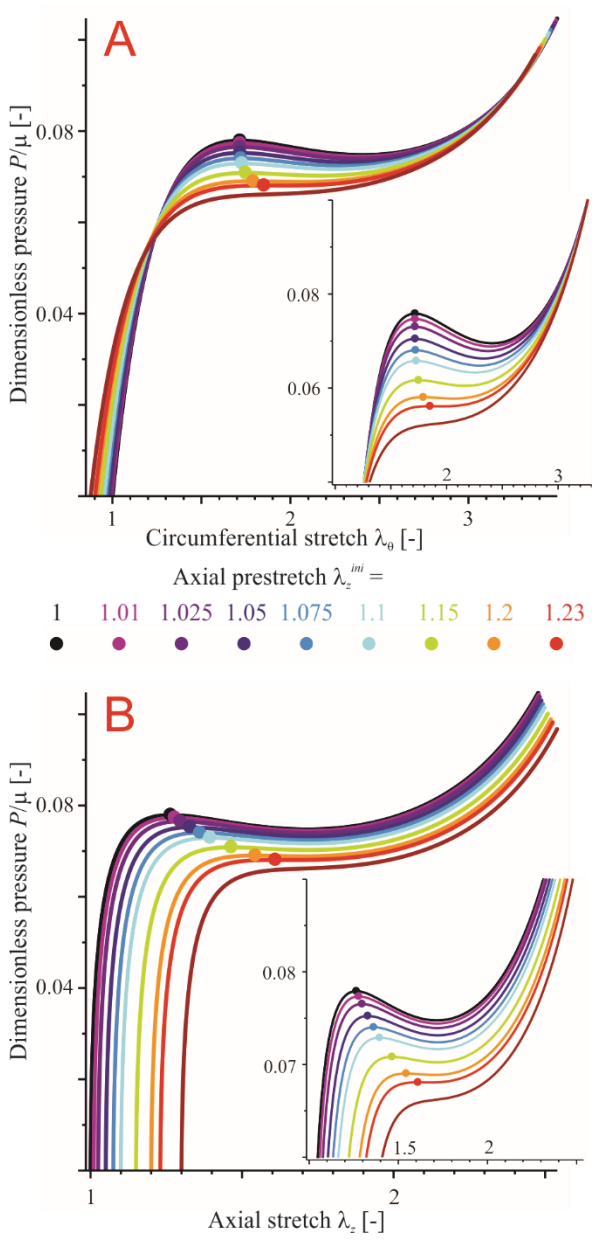

Figure 1 The inflation-extension response in **SIM1**. In SIM1, $J_m = 25$ was prescribed. Note that increased axial prestretch led to decreased P/μ and λ_θ at the onset of instability which is indicated by solid circles. For $\lambda_z^{ini} > 1.23$, the instability does not occur. The last curve, brown color, was compute for $\lambda_z^{ini} = 1.3$.

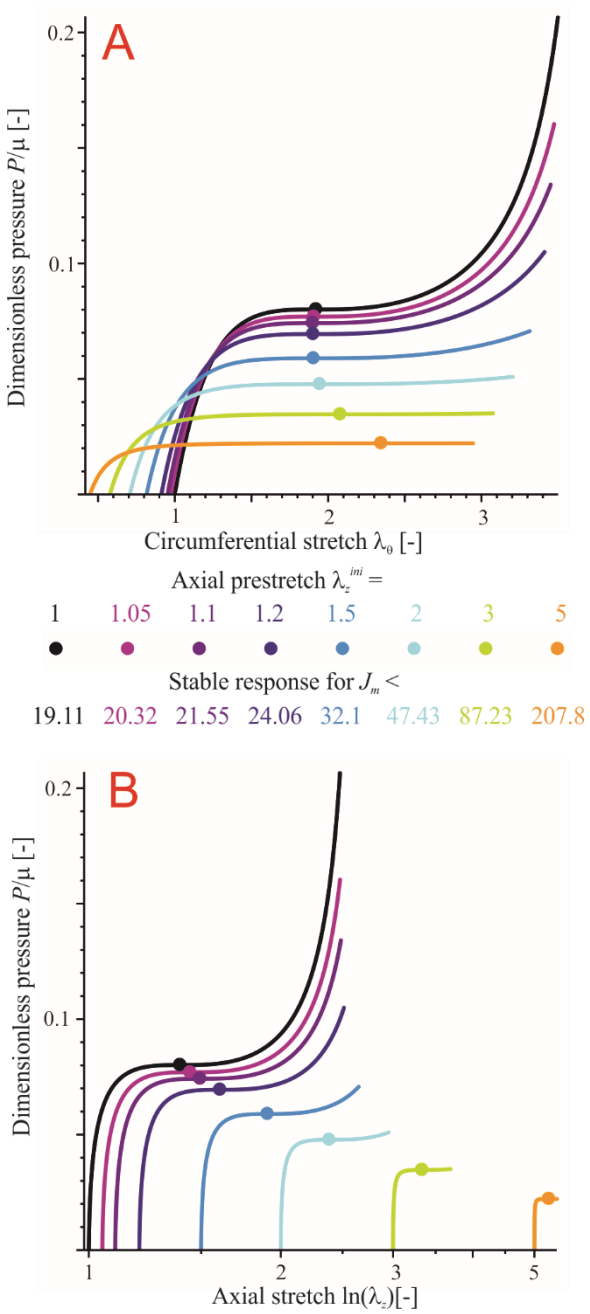

Figure 2 The inflation-extension response in **SIM2**. When tubes operate axially prestretched, they will exhibit stable response for higher J_m than in non-prestretched case. Presented values of J_m are upper bounds showing stationary point. They were obtained in the computations with λ_θ incremented by 0.001 and with four significant digits considered.

The positions of local maxima with respect to circumferential and axial stretch, normalized prestretching force and dimensionless internal pressure are detailed in the Figure 3 for **SIM1**, and for **SIM2** in the Figure 4.

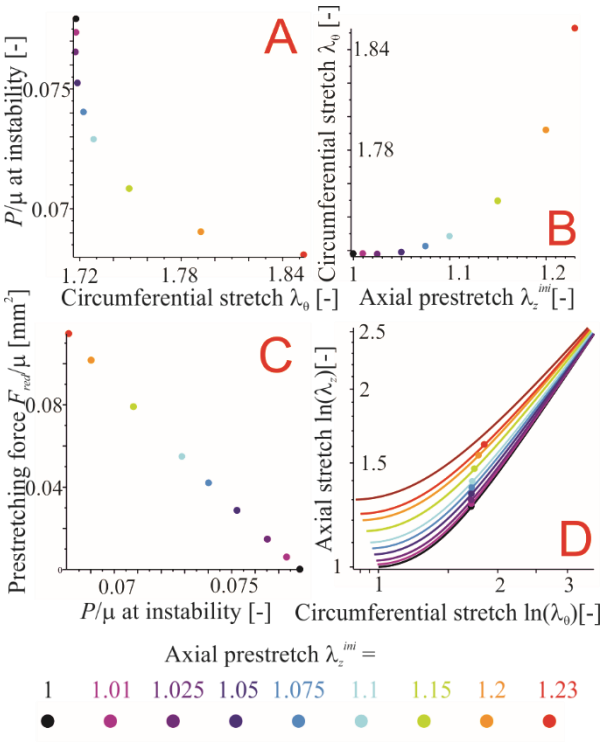

Figure 3 **SIM1** results. A – Dimensionless pressure and circumferential stretch at the local maximum. B – Circumferential stretch and axial stretch at the local maximum. C – Normalized prestretching force and dimensionless pressure at the local maximum. D – Axial and circumferential stretch during the pressurization.

The results of the simulations demonstrate that the higher the axial prestretch is, the lower is the internal pressure at which the instability occurs. The fact that local maximum pressure decreases in **SIM2** could be expected because the curves are obtained for different values of J_m. Ordinarily, J_m increases with increasing prestretretch which implies that the domain of admissible deformations extends and the material, from the certain point of view, could be regarded as more compliant. However, the pressure at local maxium decreases also in **SIM1**.

The simulations clearly demonstrate that by the imposing of the sufficient axial prestretch, finitely extensible tube is prevented from the onset of instability (**SIM1**, Figure 1). Although the internal pressure at the local maximum decreases with axial prestretch, the circumferential stretch, and thus distensibility of the tube, increases (**SIM1**, Figure 1 and 3B). In case of **SIM2**, there is, however, local minimum for $\lambda_z^{ini} = 1.1$ and $J_m = 21.55$ (Figure 4B).

The dependence of the upper bound of J_m for stable response was fitted by quadratic polynomial $J_m = 6.464(\lambda_z^{ini})^2 + 8.279\lambda_z^{ini} + 4.681$ with coefficient of determination equal 0.9999 (Figure 4A). For the sake of completeness, it should be noted that the prestetching force increases with the increment in axial prestretch.

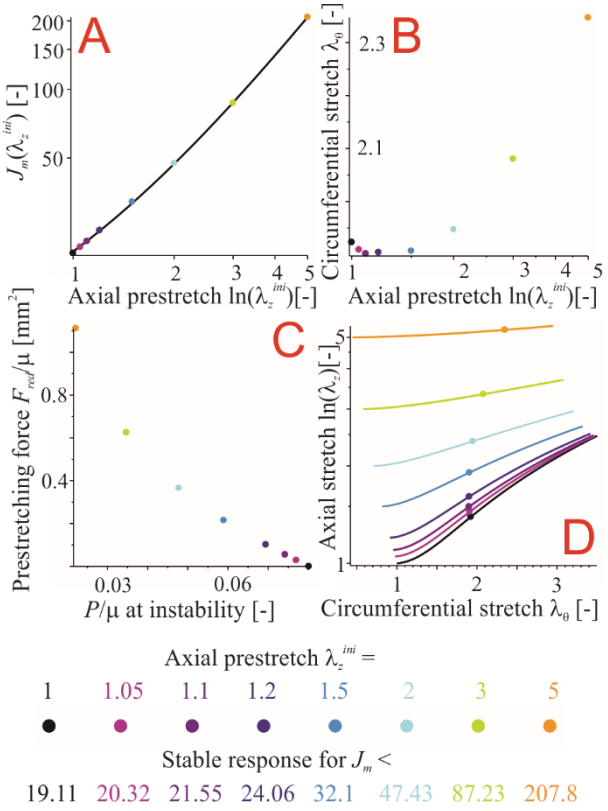

Figure 4 **SIM2** results. A – Dependence of maximum J_m with the stable inflation on axial prestretch. Obtained data is fitted by $J_m = 6.464(\lambda_z^{ini})^2 + 8.279\lambda_z^{ini} + 4.681$. B – The position of the local maxima in the circumferential and axial stretch diagram. C – Dependence of the position of local maxima on prestretching force and dimensionless internal pressure. D – Axial and circumferential stretch during the pressurization.

In contrast to Kanner and Horgan [2], minimum J_m ensuring stable response of the non-prestretched tube was found to be 19.11 (in [2] 18.2 is presented). The difference in the results comes from two sources. The first is the finite thickness of the tube entering our computation via $\varepsilon = 0.1$. Another reason for mutual mismatch is a different handling of the radial stress. In the present study, it was assumed that $\sigma_r = -\frac{1}{2}P$, however in [2] plane stress condition $\sigma_r = 0$ is used.

Finally it should be reminded that the onset of inflation instability may in experiments be accompanied with a localized deformation (bulging of the tube). Thus presented shapes of resulting curves in post-instability domain should be strictly considered as only estimates of the true behavior. Similarly to *post-buckling behavior* analyses, the determination of the true deformed geometry should leave the assumption of uniform cylindricality [12-15].

IV. ACKNOWLEDGEMENT

Present study has been supported by the Ministry of Health of the Czech Republic in the project NT13302.

REFERENCES

[1] A. N. Gent, "Elastic instabilities in rubber," *International Journal of Non-Linear Mechanics*, vol. 40, no. 2-3, pp. 165-175, 2005.

[2] L. M. Kanner, C. O. Horgan, "Elastic instabilities for strain-stiffening rubber-like spherical and cylindrical thin shells under inflation," *International Journal of Non-Linear Mechanics*, vol. 42, no. 2, pp. 204-215, 2007.

[3] M. Destrade, A. Ní Annaidh, C. D. Coman, "Bending instabilities of soft biological tissues," *International Journal of Solids and Structures*, vol. 46, no. 25-26, pp. 4322-4330, 2009.

[4] M. Destrade, R. W. Ogden, I. Sgura, L. Vergori, "Straightening wrinkles," *Journal of the Mechanics and Physics of Solids*, vol. 65, no. 1, pp. 1-11, 2014.

[5] Y. C. Fung, "*Biomechanics: Circulation*," Second edition, Springer Science+Business Media, New York, 1997.

[6] H.-C. Han, J. K. Chesnutt, J. R. Garcia, Q. Liu, Q. Wen, "Artery buckling: New phenotypes, models, and applications," *Annals of Biomedical Engineering*, vol. 41, no. 7, pp. 1399-1410, 2013.

[7] P. Badel, C. P. Y. Rohan, S. Avril, "Finite element simulation of buckling-induced vein tortuosity and influence of the wall constitutive properties," *Journal of the Mechanical Behavior of Biomedical Materials*, vol. 26, pp. 119-126, 2013.

[8] J R. Garcia, S. D. Lamm, H.-C. Han, "Twist buckling behavior of arteries," *Biomechanics and Modeling in Mechanobiology*, vol. 12, no. 5, pp. 915-927, 2013.

[9] H.-C. Han, "Nonlinear buckling of blood vessels: A theoretical study," *Journal of Biomechanics*, vol. 41, no. 12, pp. 2708-2713, 2008.

[10] H.-C. Han, "Determination of the critical buckling pressure of blood vessels using the energy approach," *Annals of Biomedical Engineering*, vol. 39, no. 3, pp. 1032-1040, 2011.

[11] J. S. Ren, J. W. Zhou, X. Yuan, X., "Instability analysis in pressurized three-layered fiber-reinforced anisotropic rubber tubes in torsion," *International Journal of Engineering Science*, vol. 49, no. 4, pp. 342-353, 2011.

[12] D. C. Pamplona, P. B. Gonalves, S. R. X. Lopes, "Finite deformations of cylindrical membrane under internal pressure," *International Journal of Mechanical Sciences*, vol. 48, no. 6, pp. 683-696, 2006.

[13] S. Kyriakides, Y. C. Chang, "On the inflation of a long elastic tube in the presence of axial lad," *International Journal of Solids and Structures*, vol. 26, no. 9-10, pp. 975-991, 1990.

[14] Y. B. Fu, S. P. Pearce, K. K. Liu, "Post-bifurcation analysis of a thin-walled hyperelastic tube under inflation," *International Journal of Non-Linear Mechanics*, vol. 43, no. 8, pp. 697-706, 2010.

[15] Y. B. Fu, Y. X. Xie, "Stability of localized bulging in inflated membrane tubes under volume control," *International Journal of Engineering Sciences*, vol. 48, no. 11, pp. 1242-1252, 2010.

[16] A. N. Gent, "A new constitutive relation for rubber," *Rubber Chemistry and Technology*, vol. 69, no. 1, pp. 59-61, 1996.

[17] C. O. Horgan, G. Saccomandi, "A molecular-statistical basis for the gent constitutive model of rubber elasticity," *Journal of Elasticity*, vol. 68, no. 1-3, pp. 167-176, 2002.

[18] C. O. Horgan, G. Saccomandi, "A description of arterial wall mechanics using limiting chain extensibility constitutive models," *Biomechanics and Modeling in Mechanobiology*, vol. 1, no. 4, pp. 251-266, 2003.

[19] L. Horny, T. Adamek, R. Zitny, "Age-Related Changes in Longitudinal Prestress in Human Abdominal Aorta." *Archive of Applied Mechanics*, vol. 83, no. 6, pp.875-888, 2013.

[20] C. S. Roy, "The elastic properties of the arterial wall," *Journal of Physiology* (London), vol. 3, pp. 125-159, 1880-1882.

[21] L. Horny, T. Adamek, E. Gultova, R. Zitny, J. Vesely, H. Chlup, S. Konvickova, "Correlations between Age, Prestrain, Diameter and Atherosclerosis in the Male Abdominal Aorta," *Journal of the Mechanical Behavior of Biomedical Materials*, vol. 4, no. 8, pp. 2128-2132, 2011.

[22] L. Horný, M. Netušil, T. Voňavková. 2013. "Axial Prestretch and Circumferential Distensibility in Biomechanics of Abdominal Aorta," *Biomechanics and Modeling in Mechanobiology*, vol. 13, no. 4, pp. 783-789, 2014.

[23] L. Horny, T. Adamek, H. Chlup, R. Zitny, "Age Estimation Based on a Combined Arteriosclerotic Index," *International Journal of Legal Medicine*, vol. 126, no. 2, pp. 321-326, 2012.

[24] A. V. Kamenskiy, I. I. Pipinos, Y. A. Dzenis, C. S. Lomneth, S. A. J. Kazmi, N. Y. Phillips, and J. N. MacTaggart, "Passive Biaxial Mechanical Properties and in Vivo Axial Pre-Stretch of the Diseased Human Femoropopliteal and Tibial Arteries," *Acta Biomaterialia*, vol. 10, no. 3, pp. 1301-1313, 2014.

[25] J. N. MacTaggart, N. Y. Phillips, C. S. Lomneth, I. I. Pipinos, R. Bowen, B. Timothy Baxter, J. Johanning, et al., "Three-Dimensional Bending, Torsion and Axial Compression of the Femoropopliteal Artery during Limb Flexion." *Journal of Biomechanics*, vol. 47, no. 10, pp. 2249-2256, 2014.

[26] A. V. Kamenskiy, Y. A. Dzenis, S. A. J. Kazmi, M. A. Pemberton, I. I. Pipinos, N. Y. Phillips, K. Herber, et al., "Biaxial Mechanical Properties of the Human Thoracic and Abdominal Aorta, Common Carotid, Subclavian, Renal and Common Iliac Arteries." *Biomechanics and Modeling in Mechanobiology*, 2014, in press.

[27] J. D. Humphrey, J. F. Eberth, W. W. Dye, and R. L. Gleason, "Fundamental Role of Axial Stress in Compensatory Adaptations by Arteries." *Journal of Biomechanics*, vol. 42, no. 1, pp. 1-8, 2009.

[28] G. A. Holzapfel, "*Nonlinear solid mechanics: A continuum approach for engineering*," John Wiley & Sons, Chichester, 2000.